Model of nonadiabatic charged-particle motion in the field of a magnetic dipole

A. N. Il'ina, V. D. Il'in, S. N. Kuznetsov, and B. Yu. Yushkov

Nuclear Physics Research Institute of Moscow State University

I. V. Amirkhanov

Joint Institute for Nuclear Research, Dubna

I. V. Il'in

Institute for Innovative and Thermonuclear Research, Troitsk

Numerical and analytical techniques are used to obtain and analyze a model for the motion of explicitly nonadiabatic particles in a dipole field, applicable to the region of stochastic instability. The basic ingredient of this model is the central trajectory (CT), a particle trajectory passing through the center of the dipole like a field line. In contrast to the generally accepted adiabatic model, in which the motion of a particle is treated with respect to a magnetic field line, here the motion is treated with respect to the CT. Approximate analytical expressions are obtained describing the CT. An iterative scheme is derived to describe the evolution of trapped particles passing through the midplane of the confinement system many times.

1. INTRODUCTION

The present problem is related to the range of applications of the theory of nonintegral systems.[1] In our case the dynamical system consists of a particle and a magnetic field. More specifically, we are concerned with particle motion in a dipole confinement system, the so-called Störmer problem for trapped particles.[2] The Hamiltonian of this system, strictly speaking, is not integrable, and so chaos, i.e., irregular motions, can occur (see, e.g., Ref. 3). Interest in a phenomenon such as deterministic chaos in magnetic systems stems from the fact that it can be the principal factor limiting plasma confinement.[4] Dipole systems attract particular attention, since in this case the solution of the problem has practical implications for space physics. For example, this applies to the dynamics of trapped particles in the magnetosphere (the Van Allen belts) of the earth.[5,6]

The stability of particle motion in a confinement geometry depends on how well the transverse adiabatic invariant (the particle magnetic moment) $\mu = mv_\perp^2/2B$ is conserved, where $v_\perp$ is the velocity component transverse to the magnetic field B. This invariant is destroyed due to the resonant interaction between the Larmor precession of the particle and its longitudinal oscillations between the mirrors of the system when the resonances overlap in phase space.[4]

There are two ways of investigating this process. The way we have chosen is based on integrating the equations of motion and calculating the change $\Delta\mu$ in the invariant over a half-period of the longitudinal oscillations.[4] The results of the calculations are interpreted on the basis of "jumps" in $\Delta\mu$ that occur when the particle crosses the midplane.[7] In this approach the quasiperiodic oscillations of μ naturally drop out of consideration.

The other approach, which is based on the Hamiltonian formalism, has certain methodological advantages.[8] By means of canonical transformations the Hamiltonian is changed to the form $H = H_0 + h$, $|h| \ll H_0$, where H_0 is the unperturbed Hamiltonian. For an axisymmetric system it has the form $H_0 = p^2/2m + \mu B(s)$, where $p/m = v_\parallel = \dot{s}$ is the parallel velocity and s is the position on a field line; the drift velocity is disregarded. The operation analogous to the determination of $\Delta\mu$ by the first approach is the identification of the resonant Fourier harmonics in the perturbation h. Then, as follows from Ref. 8, the change $\Delta\mu$ is determined by the entire particle trajectory, and not just the vicinity of the minimum B.

The effectiveness of resonant processes depends on the adiabaticity $\chi = \rho/R_c$, where $\rho = v/\omega$ is the full Larmor radius in the midplane, R_c is the radius of curvature of the field line, and ω is the gyrofrequency. In the geomagnetic field there are trapped particles with $\chi \sim 1$. For sufficiently small values $\chi \ll 1$ the magnetic moment μ is an invariant in an axisymmetric confinement system.[9] As χ increases it becomes necessary to modify (sharpen) the expression for μ by introducing correction terms from the asymptotic series for the magnetic moment.[4,10–12] However, even for $\chi \gtrsim 0.1$ the picture becomes more complicated, and higher-order terms clearly do not help.[13] The main reason for this is that the use of asymptotic series for μ (without recovering the exponential corrections, which for $0.1 \lesssim \chi < 1$ are no longer small, especially near $\chi \sim 1$ where $\Delta\mu \sim \mu$), becomes not only problematical but incorrect. Moreover, the modified expressions for μ are so complicated that it is awkward to use them in practice.

These difficulties are largely overcome through the use of the quasiadiabatic model of particle motion, which we suggested in a brief communication.[14] In this model the guiding field line is replaced by the trajectory that passes

through the center of the dipole. In consequence μ and the loss cone change. This model, in particular, yields a simple scheme for the change in μ corresponding to the concept of a discontinuous jump associated with the passage of a particle through the midplane.

In the present work we treat the quasiadiabatic model of particle motion in more detail and extend it using analytical and numerical methods.

2. STARTING EQUATIONS

The complete solution of the Störmer problem for the motion of a charged particle in the field of a magnetic dipole is only possible using numerical simulation, combining analytical and numerical techniques.

As the starting equation for the numerical calculations of single-particle orbits and the required variables on a particle trajectory we used the equation of motion in the form

$$\frac{d^2\mathbf{R}}{dt^2}=[\mathbf{v}\omega], \quad \frac{d\mathbf{R}}{dt}=\mathbf{v}, \quad \omega=\frac{e}{mc}\mathbf{B}, \quad (1)$$

where

$$B_x=-3xz\frac{M}{R^5}, \quad B_y=-3yz\frac{M}{R^5}, \quad B_z=(R^2-3z^2)\frac{M}{R^5}, \quad (2)$$

$\mathbf{R}$ is the particle radius vector (the coordinate origin is at the center of the dipole), e and $\mathbf{v}$ are the particle charge and velocity, c is the speed of light, and M is the dipole moment. At each point R a basis $\{\mathbf{e}_1,\mathbf{e}_2,\mathbf{e}_3\}$ is constructed and the velocity components are determined:

$$\mathbf{e}_1=\frac{[\mathbf{RB}]}{|[\mathbf{RB}]|}, \quad \mathbf{e}_2=[\mathbf{e}_3\mathbf{e}_1], \quad \mathbf{e}_3=\frac{\mathbf{B}}{|\mathbf{B}|}$$

$$\mathbf{v}=v_\parallel \mathbf{e}_3+v_\perp (\mathbf{e}_1 \sin \varphi+\mathbf{e}_2 \cos \varphi), \quad (3)$$

$$v_\parallel = (\mathbf{v}\mathbf{e}_3)=v \cos \alpha, \quad v_\perp =v \sin \alpha,$$

where $v_\parallel$ is the component $\mathbf{v}\parallel \mathbf{B}$, $v_\perp$ is the component $\mathbf{v}\perp \mathbf{B}$, φ is the phase measured from the meridional plane in the direction of particle rotation, and α is the pitch angle, i.e., the angle between the vectors $\mathbf{v}$ and $\mathbf{B}$. Equation (1) was integrated numerically for protons in the geomagnetic dipole field with moment $M=8.1\cdot 10^{25}$ G $\cdot$ cm^3 using a fourth-order Runge–Kutta scheme.

As is well known, in an axisymmetric field there exist two constants of motion: the energy ($mv^2=$const) and the generalized angular momentum, which for a dipole field can be written in the form

$$\frac{\cos^2 \lambda}{\tilde{R}}+\tilde{R} \sin \alpha \sin \varphi \cos \lambda=2\gamma, \quad (4)$$

or

$$\left(\frac{3}{\chi}\right)^{1/2}+\left(\frac{\chi}{3}\right)^{1/2} \sin \alpha \sin \varphi \cos^3 \lambda=2\gamma, \quad (5)$$

here $\tilde{R}=R/C_{St}=(\chi/3)^{1/2}\cos^2 \lambda$, where $C_{St}=(eM/mvc)^{1/2}$ is the Störmer length and $R=R_e\cos^2 \lambda$, where R_e

is the equatorial distance from the center of the dipole to the field line, λ is latitude, and γ is the Störmer constant determined from the initial conditions.[2] For protons in the geomagnetic field we have $C_{St}^2=5.93\cdot 10^4/p$, $=5.04\cdot 10^{-5}pcL^2$, where p is the momentum in MeV/s, $L=R_e/R_E$ specifies the field line on which the particle is located at a given moment, and R_E is the earth's radius. From (4) it follows that on the particle trajectory the following relation holds rigorously

$$R=\frac{C_{St} \cos^2 \lambda}{\gamma+\sqrt{\gamma^2-\sin \alpha \sin \varphi \cos^3 \lambda}} \quad (6)$$

for the region of finite motion for $\gamma>1$.

As shown by Amirkhanov et al.,[13] the definition $\mu=(mv^2/2B)\sin^2 \alpha$ leads to large errors for $\sin \alpha_e \lesssim \chi$, where α_e is the pitch angle in the midplane. In this case it is necessary to use for the quantity μ its expression in the laboratory coordinate system, including the transverse (magnetic) drift:

$$\mu=\frac{m}{2B} |\mathbf{v}-\mathbf{v}_d|^2 \simeq \text{const}, \quad (7)$$

where $\mathbf{v}_d$ is the first-order drift velocity.[10,15] In our variables expression (7) assumes the form

$$v_d=\frac{m}{eB} (v_\perp^2 +2v_\parallel^2) \frac{\nabla_\perp B}{B}=\frac{v\chi}{2} (1+\cos^2 \alpha)f(\lambda), \quad (8)$$

$$\mu=\frac{mv^2}{2B} \left[\sin^2 \alpha-\chi \sin \alpha \sin \varphi(1+\cos^2 \alpha)f(\lambda)\right.$$

$$\left.+\frac{\chi^2}{4} (1+\cos^2 \alpha)^2f^2(\lambda)\right], \quad (9)$$

where

$$f(\lambda)=\frac{\cos^5 \lambda(1+\sin^2 \lambda)}{(1+3 \sin^2 \lambda)^2}.$$

However, for $\chi \gtrsim 0.13$ this expression also becomes unsatisfactory.

3. THE CENTRAL TRAJECTORY AND ITS PROPERTIES

The first to draw attention to the special role of the trajectory passing through the center of the dipole was Störmer,[2] who made the assumption that this trajectory is the axis of rotation for particles near the dipole. However, subsequently this idea was not followed up.

We first describe the numerical algorithm for determining the CT and some of its properties. Then we will consider the theoretical possibilities for obtaining formulas describing the CT.

From the definition of the CT it follows that a particle must be injected from the center of the dipole along the specified field line with pitch angle $\alpha=0$ or π, depending on the hemisphere. To reduce the numerical integration, the injection point was taken on the given field line at a distance from the center of the dipole such that its position had essentially no effect on the results of the calculation. This situation was achieved even for

$R_i \lesssim (0.3–0.6)R_E(\lambda_i > 56°)$, where R_i is the distance from the dipole to the injection point, and λ_i is the latitude of this point. The numerical integration of Eq. (1) shows that the particle motion along the CT takes place almost without rotation ($v_\perp \approx v_d$). The equatorial values of the phase $\tilde{\varphi}_0 = \varphi(\lambda = 0)$ and pitch angle $\tilde{\alpha}_0 = \alpha(\lambda = 0)$ are approximated for $0.06 \leqslant \chi_i \leqslant 0.20$ by

$$\sin \tilde{\alpha}_0 = 1.4057 \chi_i^{1.1908} \exp(-0.01217/\chi_i),$$

$$\sin \tilde{\varphi}_0 = 0.1708 \chi_i^{-1.4677} \exp(-1.01162/\chi_i), \qquad (10a)$$

and for $0.20 \leqslant \chi_i \leqslant 0.75$ by

$$\sin \tilde{\alpha}_0 = 0.996 \chi_i^{0.3947} \exp(-0.1775/\chi_i),$$

$$\cos \tilde{\varphi}_0 = 1.4342 \chi_i^{-0.3765} \exp(-0.786/\chi_i), \qquad (10b)$$

where $\chi_i = \chi(R_{ei})$ is the initial value of the parameter and $R_{ei} = R_i \cos^{-2} \lambda_i$; here R_{ei} is the distance from the dipole to the point at which the given field line intersects the equatorial plane. It is noteworthy that $\tilde{\alpha}_0$ and $\tilde{\varphi}_0$ depend only on the parameter χ, which reaffirms its universality. The equatorial radius vector of a particle is determined by $\tilde{\alpha}_0$ and $\tilde{\varphi}_0$ using expression (6), which in this case assumes the form

$$R_e = \frac{2\gamma R_{ei}}{\gamma + \sqrt{\gamma^2 - \sin \tilde{\alpha}_0 \sin \tilde{\varphi}_0}}, \quad 2\gamma = \left(\frac{3}{\chi_i}\right)^{1/2}. \qquad (11)$$

The relation (11) characterizes the extent to which the CT differs from the field line ($R_e > R_{ei}$). Naturally, as $\chi_i \to 0$ the radius satisfies $R_e \to R_{ei}$, and the CT approaches closer and closer to the field line not only near the dipole, but also on the equator, where this difference is largest according to (6) and (11).

A particle moving along the CT from the dipole (CT₁) after crossing the equator turns around and is reflected at some $R > R_i$. But if the velocity vector of this particle turns through an angle equal to $\pi - \tilde{\varphi}_0$ when it arrives at the equator, leaving the pitch angle $\tilde{\alpha}_0$ unchanged, then it goes along the CT (CT₂) on the other side of the equator also. Thus, when the CT passes through the equatorial plane it undergoes a kink, characterized by the quantities $\tilde{\varphi}_{01}, \tilde{\alpha}_0$ and $\tilde{\varphi}_{02}, \tilde{\alpha}_0$. Here the phases are related by $\tilde{\varphi}_{01} + \tilde{\varphi}_{02} = \pi$ (for $\chi < 0.13$ they satisfy $\tilde{\varphi}_{01} \simeq \tilde{\varphi}_{02} \simeq \pi/2$). It turns out that the complete CT consists, as it were, of two CTs and changes discontinuously in transitions from one hemisphere to the other. In Fig. 1 the CTs are shown corresponding to the results of the numerical integration of (1). The upper and lower CT are symmetric with respect to the equator, and for them at any latitude the relations $R_1(\lambda) = R_2(\lambda)$, $\alpha_1(\lambda) = \alpha_2(\lambda)$, $\varphi_1(\lambda) + \varphi_2(\lambda) = \pi$ hold. The angular separation between the points $\tilde{\alpha}_0, \tilde{\varphi}_{01}$ and $\tilde{\alpha}_0, \tilde{\varphi}_{02}$ is determined by the quantity

$$\nu = 2 \arcsin(\sin \tilde{\alpha}_0 \sin \delta), \quad \delta = \pi/2 - \tilde{\varphi}_{01} = \tilde{\varphi}_{02} - \pi/2, \qquad (12)$$

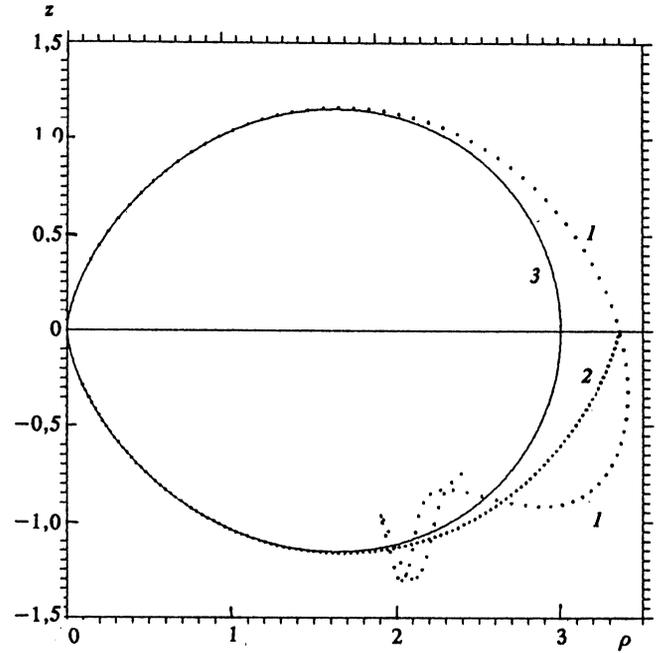for which approximate functions can be given in the form

FIG. 1. Example of the central trajectory in the meridional ρz plane ($\rho^2 = x^2 + y^2$). Injection conditions: $R_i = 0.3R_3$, $R_{ei} = 3.0R_3$, energy $W = 600$ MeV ($\chi_i \approx 0.553$). Trace 1 is the particle trajectory from the dipole to the equator and then to the reflection point in the lower hemisphere. The portion of this trajectory between the dipole (injection point) and the equator is the CT for the upper hemisphere. Trace 2 is the CT for the lower hemisphere obtained by artificially changing the particle phase on the equator, and trace 3 is the original field line.

$$\sin \nu/2 = \begin{cases} 1.36 \chi_i^{-0.044} \exp(-0.969/\chi_i), & 0.06 \leqslant \chi_i \leqslant 0.20, \\ 1.42 \chi_i^{0.053} \exp(-0.946/\chi_i), & 0.20 \leqslant \chi_i \leqslant 0.75. \end{cases} \qquad (13)$$

Now we proceed to theoretical estimates. The approximate expression for the CT was given by Störmer.[2] It was used to integrate the equation of motion by means of power series for $R(s)$ and $\cos^2 \lambda(s)$, where s is the wavelength. For R the following expression was obtained:

$$R = R_{ei} \cos^2 \lambda \left[1 + \frac{3}{8(2\gamma)^4} \left(\cos^8 \lambda + \cos^{10} \lambda \right. \right.$$
$$\left. \left. + \frac{15}{16} \cos^{12} \lambda + \frac{27}{32} \cos^{14} \lambda + ... \right) \right], \qquad (14)$$

which we write in the form

$$R = R_{ei} \cos^2 \lambda \left[1 + \frac{\chi_i^2}{24} f_s(\lambda) \right], \qquad (15)$$

where

$$f_s(\lambda) = \cos^8 \lambda + \cos^{10} \lambda + \frac{15}{16} \cos^{12} \lambda + \frac{27}{32} \cos^{14} \lambda + ...,$$

$\chi_i = 3/4\gamma^2$ [see Eq. (11)]. The principal shortcoming of Eq. (15) is the slow convergence of f_s (λ in the limit $\lambda \to 0$).

In order to find the functions $R(\lambda)$, $\varphi(\lambda)$, $\alpha(\lambda)$, and $\chi(\lambda)$ of interest to us we use Eqs. (5) and (9) and the
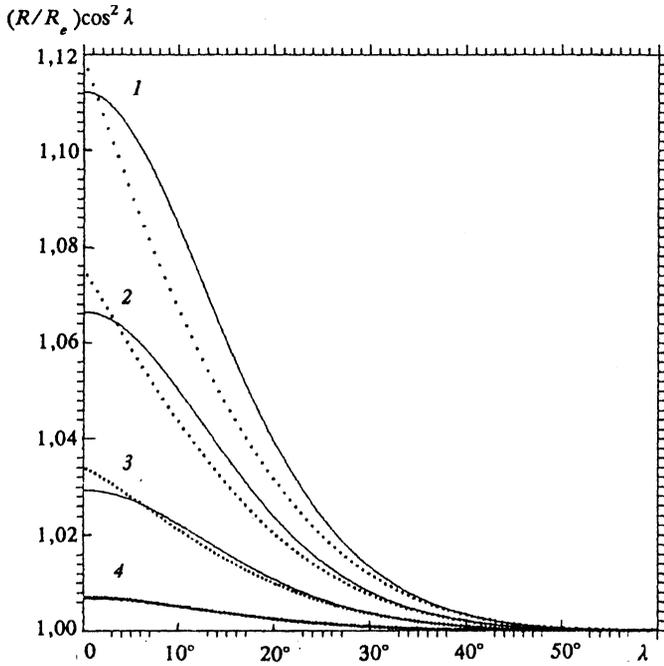
FIG. 2. Longitudinal dependence of R for the central trajectory with injection point $R_i=0.3R_3$, $R_{ei}=3.0R_3$. Results of numerical integration: trace 1 corresponds to the energy $W=600$ MeV ($\chi_i\approx0.553$), trace 2 to $W=400$ MeV ($\chi_i\approx0.433$), trace 3 to $W=200$ MeV ($\chi_i\approx0.292$), and trace 4 to $W=50$ MeV ($\chi_i\approx0.141$). The solid curves were obtained using (19).

FIG. 3. Dependence of α on λ. The notation is the same as in Fig. 2. The solid traces were obtained using (20).

natural assumption $v_\perp=v_d$ (i.e., $\mu=0$), and in a first approximation $\sin\varphi\simeq1$. Then from (9) it follows that

$$\sin\alpha=\frac{(1+2\chi^2f^2)^{1/2}-1}{\chi f}\simeq\chi f. \qquad (16)$$

Eliminating the quantity $\sin\varphi\sin\alpha$ from (5) and (9) and substituting (16) we obtain

$$\frac{\chi^2f+\tfrac{1}{4}\chi^2(2-\chi^2f^2)f^2}{(2-\chi^2f^2)f}=\frac{3}{\cos^3\lambda}\left[\left(\frac{\chi}{\chi_i}\right)^{1/2}-1\right]. \qquad (17)$$

Solving (17) by means of iterations, we find

$$\chi\approx\chi_i\left(1+\frac{2}{3}\chi_i^2f\cos^3\lambda+\frac{1}{3}\chi_i^4f^2\cos^6\lambda\right). \qquad (18)$$

It follows that

$$R=R_{ei}\cos^2\lambda\left(1+\frac{1}{3}\chi_i^2f\cos^3\lambda+\frac{1}{9}\chi_i^4f^2\cos^6\lambda\right). \qquad (19)$$

Substituting (18) in (16) we have

$$\sin\alpha=\frac{(1+2\chi_i^2f^2+\tfrac{8}{3}\chi_i^4f^3\cos^3\lambda)^{1/2}-1}{\chi_if(1+\tfrac{2}{3}\chi_i^2f\cos^3\lambda)}. \qquad (20)$$

From (5) and (20) it follows that

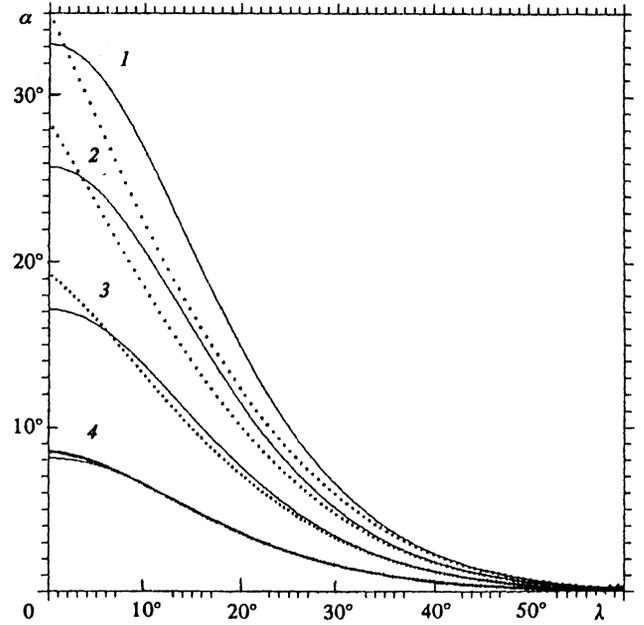$$\sin\varphi=\frac{3f[(1+\tfrac{2}{3}\chi_i^2f\cos^3\lambda)^{1/2}-1]}{\cos^3\lambda(1+\tfrac{2}{3}\chi_i^2f\cos^3\lambda)[(1+2\chi_i^2f^2)^{1/2}-1]}. \qquad (21)$$

The equatorial values $\tilde{\alpha}_0$ and $\tilde{\varphi}_0$ are obtained from (20) and (21) for $\lambda=0$. For $\chi_i\ll1$ we have [$\sin\alpha\approx\chi_if$, $\tilde{\alpha}_0\approx\chi_i$, $\sin\varphi\approx1-\tfrac{2}{3}\chi_i^2f\cos^3\lambda$, $\tilde{\varphi}_0\approx\pi/2-4\chi_i^2/3$.]. The accuracy with which Eqs. (19)–(21) describe the CT is clear from Figs. 2–4; it is $\lesssim10\%$ for $\chi_i\lesssim1.0$. Although the exact trajectory can be found only by integrating Eq. (1) numerically, nevertheless the above equations (19)–(21) enable us to obtain important information of a general nature about the properties of CT, without recourse each time to numerical methods. For example, from (19) the difference between the guide field line in the adiabatic theory ($R=R_e\cos^2\lambda$) and the CT that plays the role of the guiding center trajectory is immediately clear. It is typical that all these results depend only on λ and the parameter χ, which retain the properties of the field and particle in themselves.

4. THE QUASIADIABATIC INVARIANT

Now consider the motion of particles with initial conditions different from $\tilde{\alpha}_0$ and $\tilde{\varphi}_0$. Instead of the adiabatic invariant μ we introduce the quasiadiabatic invariant, which we define by $\mu^*=(mv^22B/\sin^2\alpha^*)$, where the quasi-pitch-angle α^* is the angle between the velocity vector and the tangent to the CT. As already noted in Refs. 13 and 14, μ^* is essentially constant on the trajectory between the reflection point and the equator, while the analogous quantity $\mu\sim B^{-1}\sin^2\alpha$ can change by several orders of magnitude. Figure 5 shows how μ^* changes on a particle trajectory over three periods of the longitudinal oscilla-
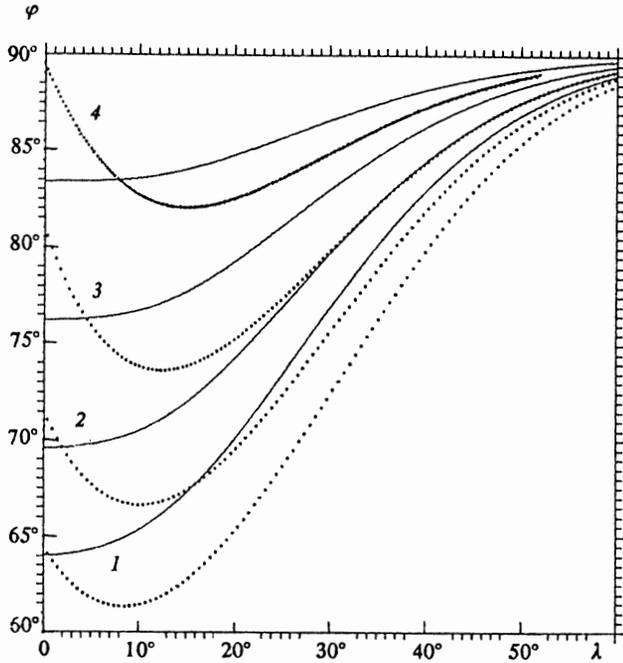
FIG. 4. Dependence of φ on λ under the same conditions as in Fig. 3. The solid curves were obtained using (21).

tions. As can be seen from the figure, it satisfies $\mu^* \simeq$ const to the left and right of the equator, and only at $\lambda = 0$ does a discontinuous change in μ^* (and hence in α^*) occur. The size of the jump is given by $\Delta \mu^* = \mu_{m_1} - \mu_{m_2} = \Delta \mu = (\Delta \mu / \mu) \mu$, where μ_m is the value of μ at the reflection
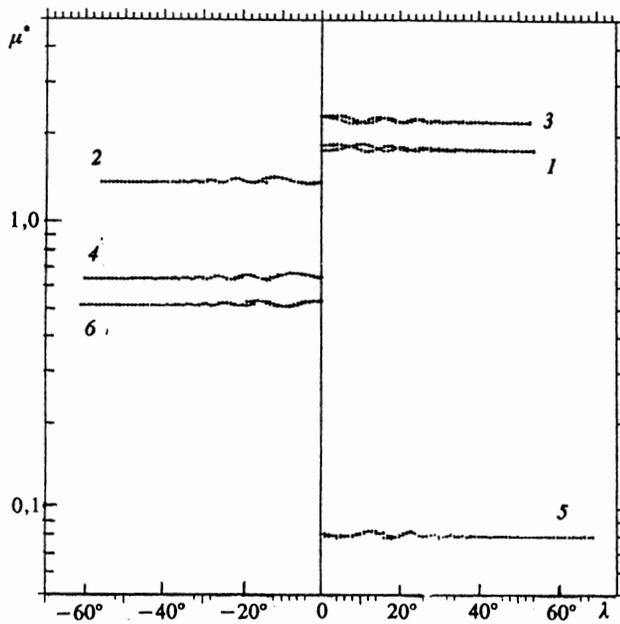

FIG. 5. Behavior of the quasiadiabatic invariant $\mu^* \sim B^{-1} \sin^2 \alpha^*$ on the particle trajectory over six reflections from the magnetic mirrors. Initial conditions: $W = 200$ MeV, $L = 2.9$ ($\chi_i \simeq 0.272$), $\alpha_0 = 19.83°$; $\varphi_0 = 71.89°$; $\lambda_0 = 0$.
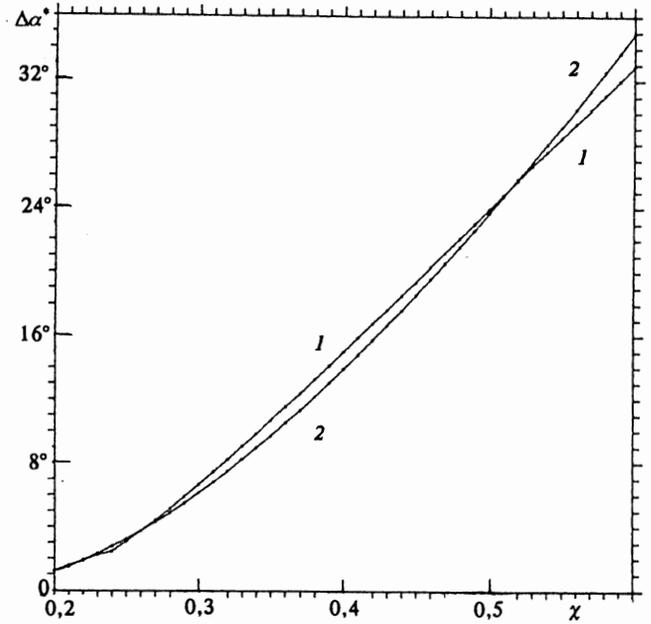

FIG. 6. Values of $\Delta \alpha^* (\phi = 0)$ as a function of χ: 1) $\Delta \alpha^* = v$; 2) $\Delta \alpha^* = \frac{1}{2} \mathrm{tg} \tilde{\alpha}_0 (\Delta \mu / \mu)_{\alpha = \tilde{\alpha}_0}$

point. This agrees to within $\sim 10\%$ with the theoretical value of $\Delta \mu$ found in Ref. 16. The value of the jump $\Delta \alpha^*$ is related to the jump v in the CT by

$$\Delta \alpha^* \simeq v \cos \varphi \simeq \frac{1}{2} \left(\frac{\Delta \mu}{\mu} \right) \mathrm{tg} \alpha, \qquad (22)$$

where $\Delta \mu / \mu$ is calculated according to Refs. 5 and 16. The accuracy of this relation is clear from Fig. 6. Expression (22) together with (13) enables us to make an additional comparison of the numerical and theoretical values of $\Delta \mu / \mu$ (Ref. 17). For example, the result of calculating $\Delta \mu / \mu$ by the method of steepest descent, taking into account the merging of the singular points (poles and saddle points[16]) yields a result very close to the numerical values.

The angle α^* increases monotonically as the particle moves from the equator toward the reflection point, where it satisfies $\alpha^* = \pi/2$. For any value of the latitude λ we have

$$\cos \alpha^* = \cos \alpha \cos \tilde{\alpha} + \sin \alpha \sin \tilde{\alpha} \cos(\varphi - \tilde{\varphi}), \qquad (23)$$

where the variables $\tilde{\alpha}$ and $\tilde{\varphi}$ refer to the CT. The change in α^*, as can be seen from the numerical experiments (see Fig. 5), is described by the adiabatic law $\sin^2 (\alpha^*/B) = $ const. This implies that between the reflection point R_m and the equatorial value α^* there exists a relation, familiar in adiabatic theory:[18]

$$\sin \alpha^* = \left[\left(4 \frac{R_e}{R_m} - 3 \right) \left(\frac{R_e}{R_m} \right)^5 \right]^{-1/4},$$

independent of the particle phase and energy. Setting $R_m = R_E$ we find

$$\sin \alpha_c^* = [(4L - 3) L^5]^{-1/4}, \qquad (24)$$

where α_c^* is the critical (limiting) value of α^* determined by the loss cone.

5. MAPPING WITH THE CT

The heading "mapping with the CT" is chosen only to emphasize the fact that the particle axis of rotation, and consequently the guiding trajectory, is the CT. Hence in a new coordinate system determined by the unit vectors $e_{1j}^*, e_{2j}^*, e_{3j}^*$, the unit vector e_{3j}^* must be directed along the tangent to the corresponding CT_j (the subscript $j = 1, 2$ indicates motion away from or toward the dipole). On the equator, as already noted, it is determined by the parameters $\tilde{\alpha}_0$ and $\tilde{\varphi}_{0j}$ which characterize the deviation of e_3^* from e_3. The unit vector e_3^* is shifted in φ clockwise for positively charged particles and in the opposite direction for negatively charged particles. The transition from the usual basis $\{e_1, e_2, e_3\}$ to $\{e_{1j}^*, e_{2j}^*, e_{3j}^*\}$ is achieved by turning the original system about e_3 in the direction of rotation and particle drift through an angle $\tilde{\varphi}_{0j}$, and then aligning the vector e_3 with e_3^* (rotation through the angle $\tilde{\alpha}_0$). In analogy with the Euler angles in analytic geometry, the transformation between the systems can be represented as

$$\cos \alpha = \cos \alpha_j^* \cos \tilde{\alpha}_0 - \sin \alpha_j^* \sin \tilde{\alpha}_0 \cos \phi_j,$$

$$\sin(\varphi - \tilde{\varphi}_{0j}) = \sin \alpha_j^* \sin \phi_j / \sin \tilde{\alpha}_0, \quad 0 \leqslant \phi \leqslant 2\pi, \quad (25)$$

where ϕ is the rotational phase measured from the plane determined by the vectors e_3 and e_3^*. From this, in particular, follows the general expression for the loss cone in the old coordinate system, which is obtained by replacing α with α_c and α^* with α_c^* in Eq. (25), where α_c^* is defined by (24). It is easy to show that even for relatively small values of $\chi (\sim 0.1)$ it is necessary to take into account the dependence of α_c on the phase φ, resulting from the particle drift.

When the trajectory crosses the equator, in connection with the change in the system of coordinates (the transformation from CT_1 to CT_2) the angular coordinates of the particle will be transformed as follows:

$$\alpha_{n1}^*, \phi_{n1} \rightarrow \alpha_{n2}^*, \phi_{n2}, \quad (26a)$$

where

$$\cos \alpha_{n2}^* = \cos \alpha_{n1}^* \cos \nu + \sin \alpha_{n1}^* \sin \nu \cos(\phi_{n1} - \tilde{\phi}_0),$$

$$\sin \phi_{n2} = \frac{\sin \nu \sin(\phi_{n1} - \tilde{\phi}_0)}{\sin \alpha_{n2}^*}, \quad (26b)$$

$$\tilde{\phi}_0 = \arcsin \frac{\sin \tilde{\alpha}_0 \sin 2\delta}{\sin \nu}.$$

After a time $\tau_2/2$ following the passage through the mirror point, the particle returns to the equator. There we have $\alpha_{(n+1)1}^* = \alpha_{n2}^*$, and the change (increase) $\Delta\phi$ of the phase can be written in the form[15]

$$\Delta\phi = \frac{\pi\bar{\omega}}{\Omega} = \frac{6F(\alpha^*)}{\chi},$$

$$\quad (27)$$

$$F(\alpha^*) \simeq \sin^{-1.348} \alpha^* - 0.255, \quad 1°.25 \leqslant \alpha^* \leqslant 90°,$$

where $\bar{\omega}$ is the Larmor frequency averaged over the longitudinal oscillation, Ω is the frequency of longitudinal oscillations, and $\chi = \chi(R_e)$. In the determination of $F(\alpha)$ the difference between the field line and the CT is disregarded, since the main contribution to the function $F(\alpha)$ comes from the integrated singularity at the reflection points,[5] where, according to (19), this difference is negligible. Finally, taking into account Eqs. (22)–(27), we arrive at heuristic mapping equations, which consist of Eqs. (26) and

$$\alpha_{(n+1)1}^* = \alpha_{n2}^*,$$

$$\phi_{(n+1)1} = \phi_n + \tilde{\phi}_0 + \frac{6F(\alpha_{(n+1)1}^*)}{\chi}. \quad (28)$$

The transformation to the usual coordinate system from the CT system is carried out using (25).

In analogy with Refs. 4 and 7, The mapping (26), (28) can be put in the form of the standard Chirikov mapping

$$I_{n+1}^* = I_n^* + K^* \sin \theta_n, \quad \theta_{n+1} = \theta_n + I_{n+1}^*, \quad (29)$$

where

$$I_n^* = \frac{3 \sin \alpha_r^*}{\chi} \left(\frac{\sin^2 \alpha^* - \sin^2 \alpha_r^*}{\sin^2 \alpha_r^*} \right) \left(\frac{\partial F}{\partial \sin \alpha^*} \right)_{\alpha_r^*},$$

$$K^* = \frac{6\nu}{\chi} \left| \frac{\partial F}{\partial \alpha^*} \right|_{\alpha_r^*},$$

K^* is the stochasticity parameter, $\theta = \phi - \tilde{\phi}_0 - \pi/2$, and α_r^* is found from the resonance condition $\bar{\omega} = 2r\Omega$) (here $r = \bar{\omega}/2\Omega = 3F/\pi\chi$ is an arbitrary whole number). For the mapping in the usual coordinate system[7] $[(I(\alpha)_n \rightarrow I(\alpha)_{n+1}, \chi \ll 1]$ the stochasticity parameter assumes the form

$$K = -\frac{1.52(14 - \sin^2 \alpha)}{\chi \cos \alpha \sin^{2.348} \alpha} \exp\left[-\frac{3\psi(\alpha)}{\chi} \right], \quad (30)$$

where

$$\psi(\alpha) = \frac{1}{3\sqrt{2} \sin^2 \alpha} \left(\frac{1 + \sin^2 \alpha}{\sin \alpha} \ln \frac{1 + \sin \alpha}{\cos \alpha} - 1 \right).$$

The expression for $\psi(\alpha)$ after the transformation is taken from Ref. 16. The boundary of the region of global stochasticity, determined from the condition $K^* = 1$ or $K = 1$ (Refs. 4 and 7) is shown in Fig. 7. For comparison two versions are shown.

As is well known, the reason for using discrete models of the motion is that they permit long-term predictions to be made over a time $\sim 10^6$ periods of the longitudinal particle oscillations. Furthermore, they make it very easy to distinguish stationary, quasiperiodic, and chaotic motions. This model works efficiently for $\chi_i < 1$ and $\alpha^* \lesssim 45°$, which corresponds to the region of the stochastic instability (see Fig. 7).

A more precise estimate of the boundary of the region of applicability for the model with a CT can be obtained from the following considerations. On the equator the drift
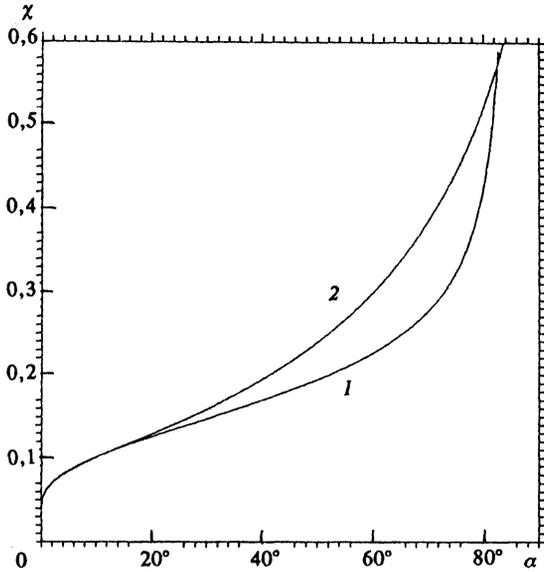
FIG. 7. Boundary of stochasticity: *1*) $K^*=1.0$; *2*) $K=1.0$.

velocity of a particle moving on the CT is equal to $[v_{dc} \simeq \chi/2(2-\sin^2\tilde{\alpha}_0)v]$ according to (8), while for a particle with arbitrary pitch angle we have $[v_d \simeq \chi/2(2-\sin^2\alpha)v]$. From the condition that these two drift velocities agree to better than 10% we find using (20)

$$-0.2+1.1\chi_i^2+0.37\chi_i^4 \lesssim \sin^2\alpha \lesssim 0.2+0.9\chi_i^2+0.3\chi_i^4. \tag{31}$$

For $\chi_i \lesssim 0.416$ we have $\alpha_{min}=0$; α_{max} is determined from the condition (31). For $\chi \simeq 0.416$ we have $\alpha_{max} \simeq 37°$. This condition corresponds to an important physical case, in which particles are close to the loss cone, i.e., they have reflection points near the surface of the earth.

In this case simple analytical estimates can be made of the particle lifetime from the diffusion equation:[4]

$$\frac{d}{d\mu}\left(D_\mu \frac{df}{d\mu}\right)+q(\mu)=0.$$

Here the diffusion rate is

$$D_\mu=\left(\frac{\overline{\Delta\mu}}{\mu}\right)^2\mu,$$

where the superior bar indicates averaging over phase, $f(\mu)$ is the distribution function, $q(\mu)=\mu^\beta$ is the source density, and $\beta>-1$ is a constant. Using the standard procedure,[4] we obtain

$$\tau_n \approx 0.15 \exp\left(\frac{6\psi}{\chi}\right)\sin^2\alpha_{St} \ln\frac{\sin\alpha_{St}}{\sin\alpha_c}, \quad \alpha_{St} \gg \alpha_c, \tag{32}$$

where τ_n is expressed in terms of the number of passes of the particle between the mirror points, α_{St} corresponds to the boundary of stochasticity $K=1$ (see Fig. 7), and $6\psi/\chi \approx 2$ for $\alpha \ll 1$. In the system with the CT, taking into account (23) instead of (32), we find

$$\tau_n=\frac{\sin^2\alpha_{St}^*}{\nu^2}\ln\frac{\sin\alpha_{St}^*}{\sin\alpha_c^*}, \tag{33}$$

where α_{St}^* is determined from the condition $K^*=1$ and α_c^* is the value of α^* on the adiabatic loss cone [cf. Eq. (22)]. To switch from discrete time to continuous we must multiply (32) and (33) by the average value π/Ω.

6. CONCLUSION

To conclude our analysis of the model of motion for the nonadiabatic case we note that using the CT enables us to retain in a modified (relabeled) form the main ideas of the adiabatic theory. This is expressed verbally in the addition of the prefix "quasi" to the words defining μ^* and α^* in particular. Ultimately it is found that this model of the motion includes the adiabatic motion (μ^*=const) between the equator and the reflection point and back and the discrete model (26), (28), or (29) for multiple longitudinal particle oscillations. As a whole the model of the motion can be called "the CT model," and its discretized part can be called "mapping with the CT." For $\chi\to0$ the model with the CT goes over to the adiabatic model with the corresponding guiding field line. These results may be useful for studying the dynamics of particles in confinement systems with different types of magnetic field geometry.

[1] V. I. Arnol'd, A. I. Kozlov, and A. I. Neishtadt, *Mathematical Aspects of Classical and Celestial Mechanics: Current Problems of Mathematics, Fundamental Directions*, Vol. 3 [in Russian], VINITI, Moscow (1985).
[2] C. Störmer, *The Polar Aurora*, Clarendon Press (1955).
[3] C. Jung and H.-J. Scholz, J. Phys. A: Math. Gen. **21**, 2301 (1988).
[4] B. V. Chirikov, in Reviews of Plasma Physics, Vol. 13, B. P. Kadomtsev (ed.), Consultants Bureau, New York (1987).
[5] V. D. Il'in and A. N. Il'ina, Fiz. Plazmy **8**, 148 (1982) [Sov. J. Plasma Phys. **8**, 83 (1982)].
[6] V. D. Il'in, I. V. Il'in, and S. N. Kuznetsov, Kosm. Issled. **24**, 88 (1986).
[7] B. V. Chirikov, Fiz. Plazmy **4**, 521 (1978) [Sov. J. Plasma Phys. **4**, 289 (1978)].
[8] A. V. Zvonkov and A. V. Timofeev, Fiz. Plazmy **11**, 320 (1985) [Sov. J. Plasma Phys. **11**, 186 (1985)].
[9] V. I. Arnol'd, Usp. Mat. Nauk **18**, No. 6, 91 (1963) [Usp. Mat. Nauk].
[10] T. G. Northrop, *The Adiabatic Motion of Charged Particles*, Wiley, New York (1963).
[11] A. J. Lichtenberg, *Phase Space Dynamics of Particles*, Wiley, New York (1969).
[12] V. I. Il'gisonis, Zh. Eksp. Teor. Fiz. **101**, 58 (1992) [JETP Lett. **74**, 31 (1992)].
[13] I. V. Amirkhanov, A. N. Il'ina, V. D. Il'in, and B. Yu. Yushkov, Kosm. Issl. **29**, 282 (1991).
[14] V. D. Il'in, I. V. Il'in, S. N. Kuznetsov, and B. Yu. Yushkov, Pis'ma Zh. Eksp. Teor. Fiz. **55**, 621 (1992) [JETP Lett. **55**, 645 (1992)].
[15] S. I. Braginskii, Ukr. Mat. Zh. **8**, 119 (1956).
[16] V. D. Il'in and A. N. Il'ina, Zh. Eksp. Teor. Fiz. **75**, 518 (1978) [JETP Lett. **48**, 259 (1978)].
[17] I. V. Amirkhanov, E. P. Zhidkov, A. N. Il'ina, and V. D. Il'in, Report P11-85-88, JINR, Dubna (1985).
[18] H. Roederer, *Dynamics of Radiation Trapped by the Geomagnetic Field* [Russian translation], Mir, Moscow (1972).

Translated by David L. Book